



# Recyclable electroactive paper based on cationic fibers adaptable to industrial papermaking

Alireza Hajian · Karishma Jain · Nuzhet Inci Kilic · Artem Iakunkov · Chandrasekar M. Subramaniyam · Lars Wågberg · Per A. Larsson · Mahiar Max Hamedi

Received: 1 March 2024 / Accepted: 15 August 2024 / Published online: 26 August 2024  
© The Author(s), under exclusive licence to Springer Nature B.V. 2024

**Abstract** Paper is the largest renewable industrial substrate produced for various applications and can be recycled by disintegrating the fibers and reforming the paper. Paper and its fiber constituents lack functions such as electrical conductivity and papermaking itself has not been used for producing electronic devices. In this work, we show a potential industrially viable route for introducing cationic charges on the cellulose fibers and subsequently show how the adsorption of negatively charged ionically and electrically conductive materials onto these fibers from

aqueous media can be applied at time scales relevant to industrial papermaking. This results in electroactive fibers, that can subsequently be used to prepare electroactive papers using standard papermaking procedures. Since fibers in the paper can selectively be coated with different active materials, various functions can be added into the paper. To demonstrate applications, we prepared electroactive papers using fibers with adsorbed carbon nanotubes (CNTs) and conducting polymers. We achieved conductivity of 21 S/m with only 1wt% CNT. We also prepared papers with CNTs and black phosphorus, used as paper-based lithium, and sodium ion battery (free-standing) anodes. They delivered a specific capacity of 642 mA h g<sup>-1</sup> at 100 mA g<sup>-1</sup> after 3500 cycles with 99.5% columbic efficiency. Furthermore, we recycled the papers, and as the disintegration of the fibers did not lead to removal of the ionic or electroactive materials from the fiber surface, the recycled papers showed similar electrical and mechanical properties to the original papers. This opens the path for recyclable paper-based electronics.

<sup>†</sup>Karishma Jain and Nuzhet Inci Kilic have contributed equally.

**Supplementary Information** The online version contains supplementary material available at <https://doi.org/10.1007/s10570-024-06128-9>.

A. Hajian (✉) · K. Jain · N. I. Kilic · A. Iakunkov · C. M. Subramaniyam · L. Wågberg · P. A. Larsson · M. M. Hamedi (✉)  
Department of Fiber and Polymer Technology, KTH Royal Institute of Technology, 10044 Stockholm, Sweden  
e-mail: hajian@kth.se

M. M. Hamedi  
e-mail: mahiar@kth.se

*Present Address:*

C. M. Subramaniyam  
Chemistry and Biochemistry Dpt., Facultad de Farmacia, Universidad San Pablo-CEU, CEU Universities, Urbanización Montepríncipe, 28668 Boadilla del Monte, Madrid, Spain

**Keywords** Paper · Fiber · Battery · Recycle · Composite · Adsorption

## Introduction

The worldwide production of cellulose fibers from trees is currently very large, reaching an annual

paper production of around 400 million metric tons. (Przybysz et al. 2018) Most of these fibers are used in paper making primarily for packaging, hygiene and printing products, making it one of the largest substrates that is industrially produced from a renewable resource. Cellulose-rich papers are made by dewatering of the wet fibers on large scale paper machines at speeds exceeding 1500 m/min, resulting in a random-in-plane oriented fibrous network. In paper, the fiber–fiber contacts define its main mechanical as well as transport/transfer properties, such as stress, strain and heat. (Yi et al. 2004; Picu 2011).

Pristine papers lack active functions such as heat and electrical conduction, or biological functionality, required for different advanced high-value applications. For this reason, different approaches have been used to add functions primarily by adding inks, like electroactive inks, metals, bioactive inorganic materials or biopolymers, onto a prefabricated paper using techniques like screen printing, roll-to-roll, or digital print/press. (Martinez et al. 2007; Hu et al. 2009, 2010; Hübler et al. 2011; Hamedí et al. 2016; Lin et al. 2016) These have resulted in two major categories of multifunctional paper: (i) Printed electronics, which is currently done by adding electroactive inks onto or into dry paper to form electronic devices like digital electronics, displays, solar cells, and batteries. (Berggren et al. 2007; Tobjörk and Österbacka 2011; Hu and Cui 2012; Pettersson et al. 2014; Brunetti et al. 2019) (ii) Paper microfluidic analytical systems also known as  $\mu$ PADs, where hydrophobic regions are printed into paper to create microfluidic structures, followed by printing of biomolecules and reagents for the fabrication of biomolecular analytical systems. (Yamada et al. 2015; Hamedí et al. 2016).

Adding functions to prefabricated paper, however, has four major problems limiting its possibilities: (i) de-watering forms closed contacts at the fiber junctions, thus making the fiber contacts less accessible to penetration of inks. The fiber is furthermore already in a dry-state and wet adsorption on to the dry fibers cannot be fully utilized. (ii) It is not possible to fabricate composite papers in which a single fiber carries different functional materials to an adjacent fiber. (iii) The additional steps posterior to papermaking require other machines and factories, thus causing a substantial added cost and hence a significant barrier to implementation. Furthermore, since most papers are inhomogeneous in the thickness, it is difficult to print

well-defined thin films on an uncoated paper. (iv) The recycling of paper with functional materials added on top is challenging, as the functional inks should be removed in a separate process to that of paper recycling. (Hu et al. 2010; Leijonmarck et al. 2013; Nguyen et al. 2014) Furthermore, paper electronics without a feasible recycling route do not necessarily have advantage over printed circuit boards. (Sudheshwar et al. 2023).

To solve these problems one approach has been to incorporate functional particles of similar size to that of the fiber itself, such as carbon fibers or graphite, to the wet fiber prior to papermaking to make composite papers; this method provides a two-phase system where cellulose fibers only act as the skeleton and do not adsorb the particles evenly distributed on the fibers. (Mirica et al. 2013; Kaplan et al. 2017; Isacson et al. 2020) Another approach involves the modification of the cellulose fibers of prefabricated paper using adsorption or chemistry, followed by adsorption of particles or polymers. This approach might be complex with treatment steps mainly suitable for the preparation of a single material/function. (Fugetsu et al. 2008; Imai et al. 2010; Koklukaya et al. 2015).

In the present approach for fiber treatment, we solve all the four major issues listed above. Our solution relies on a potential industrially scalable chemical modification of fibers, which introduces cationic charges on the surface of the fibers in wet state. These fibers can subsequently adsorb numerous negatively charged functional materials ranging from conducting polymers to nanomaterials like carbon nanotubes (CNTs) turning the wet fibers into functional fibers. They can then be used alone or in mixtures in a conventional paper-making process to form a fundamentally new form of functional paper at scale. (Isacson et al. 2022) This is possible because the adsorbed materials are not washed away from the fibers during the dewatering process, and do not necessarily disrupt the formation of strong fiber contacts resulting in papers with acceptable mechanical properties. Furthermore, a lot can be achieved at modest addition levels and the adsorbed amount is only around 1 wt% of the dry paper composite. Here, individual fibers can also carry individual function that is different from the adjacent fibers and form intimate connections in the paper network once the percolation threshold has been passed. The fiber junction of these papers thus both forms a strong network to provide

strength and acts as a connection point for the electronic transport between the fibers, provided the modification has been performed with care and skill.

## Materials and methods

### Preparation of cationic fibers

For the preparation of cationic cellulose fibers, the previously reported method by Pei et al. (Pei et al. 2013) was used with slight modifications. A softwood sulfite dissolving pulp (100 g dry, Domsjö Fabriker AB, Sweden) was mixed with 4.78 M NaOH and left for 10 min to activate the surface hydroxyl groups of cellulose. A dissolving pulp was chosen because it has few impurities and is rich in cellulose (93–95% cellulose), facilitating a defined system for small-scale studies. It should be noted that other bleached pulps, with higher hemicellulose content, would perform similarly.

Afterward, isopropanol (153 g, Sigma Aldrich) and glycidyl trimethylammonium (100 g, 99.9% purity, Sigma Aldrich) were added to the activated fibers and mixed thoroughly. The reaction was carried out at 65 °C for 6 h in a hot water bath. Subsequently, the reaction mixture was neutralized with 1 M hydrochloric acid (Sigma Aldrich), filtered, and washed thoroughly with DI water using vacuum filtration. The charge density of the fibers was measured using polyelectrolyte titration, and the estimated charge density was  $250 \pm 50 \mu\text{eq/g}$ .

### Preparation of black phosphorus

Commercial red phosphorus chunks (of 99.9% purity) were purchased from Sigma Aldrich and hand ground to powder using mortar pestle. The black phosphorus (BP) nanomaterials were obtained by ball milling of red phosphorus powders under inert atmosphere. The red phosphorus powder was dried in vacuum oven at 60 °C for 24 h and then transferred to argon-filled glove box maintained at  $<0.1$  ppm of  $\text{O}_2$  and  $\text{H}_2\text{O}$ . The red phosphorus was subjected to high energy ball milling using tungsten-carbide vials and balls at 300 rpm with ball to powder weight ratio of 20:1, respectively, for 20 h in Retsch PM 400 ball mill. The obtained black powders were collected and processed

inside glovebox so as to avoid contamination due to self-ignition as ball milled powders are highly reactive upon contact with atmospheric air.

### Coating (saturating) the fibers with nanomaterials

A cationic fiber dispersion (2 g/L) in water was prepared (fiber dry weight 0.5 g), and 50 mg (measured dry weight) of either poly(3,4-ethylenedioxythiophene) polystyrene sulfonate (PEDOT:PSS) or single-wall carbon nanotubes (SWNTs) from aqueous dispersion (1 g/L) was added to this dispersion. PEDOT:PSS (ICP 1050) were purchased from Agfa and the carboxylic acid functionalized SWNTs (P3-SWNTs > 90% purity) were purchased from Carbon Solutions Inc. The mixture was stirred using an overhead stirrer for 30 min. Here, the fiber concentration as well as the PEDOT or SWNT concentrations are known. Next, 10 mL (using a plastic syringe) from the mixture was picked and filtered out the unadsorbed PEDOT:PSS or SWNT in a vial—got a clear blue or gray dispersion. Then, the dried weight was measured to obtain the concentration of the unadsorbed PEDOT:PSS or SWNTs. By subtracting that from the original PEDOT:PSS or SWNT concentration in the fiber-water mixture, the adsorbed amount was calculated. This procedure was repeated 5 times to get an average data point. The PEDOT:PSS or SWNTs (dry weight percent adsorbed) varied somewhat between 0.5 wt% and 1.5 wt%.

### Dynamic light scattering (DLS)

Zetasizer ZEN3600 (Malvern Instruments Ltd., UK) was used. Disposable polystyrene cuvettes were filled with sample to a volume of 2 mL in each cuvette. Measurements were performed at 25 °C and each curve is the average of 10 s measurements. Based on the settings, each measurement was repeated 5 times for each sample to enable averaging and normalized intensity correlation function versus time of each sample was obtained. The hydrodynamic diameter of the BP and SWNTs in pure water, as well as the zeta potential were recorded.

### Tensile testing

Tensile testing of the papers was done using Universal Material Testing Machine Instron 5944 (Norwood,

MA, USA) equipped with 500 N load cell, cross-head speed of 5 mm/min (strain rate of 10%/min). 5 specimens from each paper were cut into rectangles having the length of 5 cm and width of 5 mm and tested (to enable averaging). All the tensile tests, and other measurements on dried papers and fibers were done in a controlled condition room having constant temperature of 23 °C and a constant relative humidity of 50%. All the papers were conditioned for 24 h prior to measurement.

#### Fabrication of the composite papers and paper sheets

The coated fibers were mixed in a given ratio in water, and mixed for 5 min using an overhead stirrer. All the papers (with coated fibers or not coated) were prepared using tap water in a Rapid Köthen equipment (Paper Testing Instruments, Austria). The sheets were dried at 93 °C under a reduced pressure of 95 kPa for 10 min. The apparent density of the papers was measured in the range of 725–760 kg/m<sup>3</sup>.

#### Scanning electron microscopy (SEM) imaging

SEM images were captured using the high-vacuum field-emission SEM (Hitachi S-4800, Hitachi Corp., Japan). The samples were fixed on a metal stub and sputtered with 5–6 nm layer of gold–palladium using Cressington 208HR (Watford, UK).

#### Conductivity measurement of individually coated fibers

The conductivity of the coated fibers was measured by drying individual fibers on a glass plate, painting the two ends side of each fiber with conducting silver paint, and measuring the resistance of the fiber using two point probe resistance measurement (KEITHLEY, Beaverton, USA) from these silver contacts.

The length and width of each fibers was calculated using image analysis of microscopy photos taken with a Zeiss “Stemi” microscope. These values were used to normalize the resistance/square value for each fibers. See Table S1.

#### Conductivity measurement on composite papers

The electrical conductivity of the papers was measured using a two-point probe technique. The papers were cut into rectangular shapes 5 mm wide and 5 cm long. The two edges of the papers were silver painted to provide good contact between the metal probe and the paper. The electrical resistance of each paper was measured using Source Meter 2401 (KEITHLEY, Beaverton, USA).

#### Battery test

The multifunctional composite paper was tested as free-standing and additive-free negative electrode in a half-cell configurations against Li and Na metals, respectively, for lithium-ion and sodium-ion batteries. The free-standing composite paper was disc-cut to 12 mm diameter and directly used as anode for lithium and sodium-ion batteries. A half coin cell configuration constituting of composite paper as working electrode and lithium metal disc as counter/reference electrode partitioned by Celgard 2200 grade separator impregnated with 1 M LiPF<sub>6</sub> in 1:1 (v/v) EC:DEC electrolyte was fabricated in an argon-filled glove box maintained at <0.1 ppm O<sub>2</sub> and <0.1 ppm H<sub>2</sub>O. The fabricated cells were rested overnight and electrochemically tested at specific current density between 0.002 and 3 V against Lithium in a multichannel battery tester (Lanhn battery Inc., China). The impedance spectra of the fresh cells were tested at 5 mV amplitude between 0.1 and 10 mHz frequencies using BioLogic VMP3 Instruments, France. Similarly, for sodium cells, 1 M NaPF<sub>6</sub> in 1:1 (v/v) EC/DEC + 10% FEC as electrolyte and Whatsmans (G/F) grade as separator between the working electrode (composite paper) and sodium metal disc (counter/reference electrode). The sodium cells were cycled between 0.002 and 2 V at specific current density (mA/g). The specific capacity (mAh/g) was calculated based on the wt.% of black phosphorus and CNT combined.

#### T-cell configuration

Recycled and non-recycled 100% SWNT/CNT papers were characterized in a three-electrode setup with a T-cell configuration, where reference and counter electrodes were Ag/AgCl (3 M KCl) and activated

carbon mixture, respectively and separated via monolayer microporous polypropylene membrane. Electrolytes with a 1 M concentration, containing H<sub>2</sub>SO<sub>4</sub> (in water) and 1 M tetraethylammonium (in acetonitrile), were subjected to testing. In the case of the non-aqueous electrolyte, the T-cells were assembled inside a glovebox Lab star eco (MBraun, Germany) in argon atmosphere (H<sub>2</sub>O < 0.5 ppm and O<sub>2</sub> < 0.5 ppm).

### Electrochemical characterization

The electrochemical performance of the papers was evaluated with cyclic voltammetry (CV) and recorded with VSP potentiostat (Bio-Logic Cromocol Scandinavia, Sweden). Moreover, cyclic charge–discharge stability tests were also performed using Landt instruments battery testing system (CT2001A, Landt Instruments, USA). For the measurement with T-cell configuration, CV measurement was performed in three electrode configurations. CV measurements were recorded at scan rates from 5 to 500 mV/s under 0 to 1 V and –0.6 to 1 V potential window in aqueous and non-aqueous electrolytes, respectively.

Capacitance values were extracted from the forward CV scan curves for each scan rate, where the area under the curve represents the charge accumulated in the device with voltage increase. Subsequently, by relating charge and capacitance ( $C = Q/V$ ; C is capacitance, Q is charge, and V is voltage), specific capacitance values were extracted for all the samples in both organic and inorganic electrolytes using the following equation;

$$C = \frac{\int IdV}{v\Delta V}$$

where the numerator represents the area under the curve of forward scan (anodic scan),  $v$  and  $\Delta V$  represent scan rate and potential window respectively.

In CV measurements, a potential window of –0.6 to 1 V for organic and 0 to 1 V for inorganic electrolyte was used. Exceeding the used voltage window resulted in observation of the development of high redox current related to decomposing the electrolyte. Consequently, the optimized potential working window has been selected to ensure the reliability and accuracy of our results.

### Recycling the papers

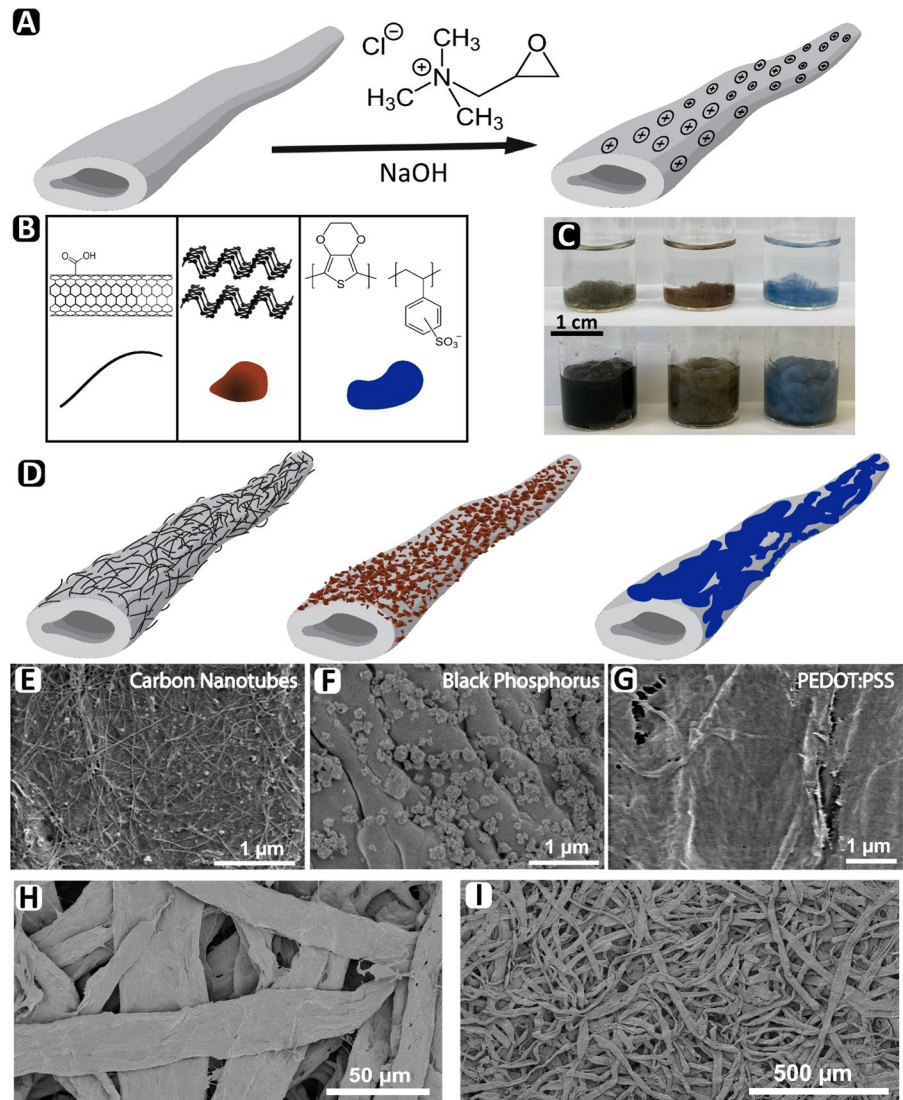
For recycling, a similar method as for making the composite papers was used. The sheets were first soaked in DI water overnight and slushed at 10,000 rpm in a mechanical slusher. Next, Rapid Köthen sheet former was used at 93 °C under a reduced pressure of 95 kPa for 10 min.

### Results and discussion

The major industrial routes for large scale fiber production involve chemical and mechanical treatments. Fibers from fully delignified wood usually have a low surface charge and can therefore only adsorb a limited amount of oppositely charged functional materials through self-assembly in water. (Agarwal et al. 2009) To solve this problem, we prepared cationically charged cellulose fibers, using a similar method to that used for cationic starch in industry. This method in short involves the conversion of alkali-activated surface hydroxyl (-OH) groups on cellulose to quaternary ammonium groups by reaction with glycidyl-trimethylammonium chloride (Pei et al. 2013; Ho et al. 2011) (see Fig. 1A). This chemical route results in an estimated fiber charge of around 300  $\mu\text{equiv/g}$ . These charged groups further enable an efficient adsorption of anionically charged materials onto the cellulose fibers in aqueous media, at a concentration below 1 wt%, and with a dewatering time of less than 1 min which is required for industrial papermaking. Our fibers therefore open the path of adding numerous functional materials onto the fibers by simply adding a pretreatment step prior to paper making.

The majority of functional materials (especially conducting polymers, 1D, and 2D materials) are negatively charged which aids in their dispersion in water. They can therefore adsorb homogeneously onto the cationic fiber in water. We have chosen several of the most important electroactive materials; single-wall carbon nanotubes (SWNTs), black phosphorus (BP) of irregular-shape, and the conducting Poly(3,4-ethylenedioxythiophene):poly(styrenesulfonate) (PEDOT:PSS), all dispersed and stabilized in water, to coat the cationic fibers by mixing these materials with the fiber suspension. This was simply achieved by adding the dispersion to the fiber-water mixture during stirring and after 30 min the fibers

**Fig. 1** Schematic diagrams showing **A** the cationization of the fibers. **B** The active nanomaterials used here to adsorb on cationic fibers (from left to right: single wall carbon nanotubes, black phosphorus, PEDOT:PSS). **C** Optical images from wet cationic fibers coated with (from left to right) SWNT, black phosphorus, PEDOT:PSS, at 1 g/L (top) and 10 wt% (bottom). **D** Their respective schematics. SEM images from fiber surfaces coated with **E** SWNTs, **F** Black phosphorus, **G** PEDOT:PSS. **H** and **I** SEM images from the fiber network at different magnifications



were dewatered which resulted in a 10 wt% wet fiber pad in which the coated material constituted around 1 wt% of the solid content (see Fig. 1 and Figure S1).

By mixing uncoated and coated wet fibers at different ratios we could also prepare a number of different composite papers. To show a major advantage of our paper making process for multifunctional papers, we demonstrate that these papers are easily recyclable. We recycled the composite papers, containing 5% to 100% coated fibers (either with PEDOT:PSS or SWNTs), by re-dispersing the papers into fibers in water (see Fig. 2A). Figure 2B shows examples of papers containing different amounts of functional

fibers coated with PEDOT:PSS or SWNTs (ranging 5–100% coated fibers).

The maximum conductivity of SWNTs composite papers (21.7 S/m) was around ten times higher than the PEDOT:PSS papers (2.8 S/m), at the highest fraction (see Table S2). This can be attributed to the formation of a denser network of particles alongside each fiber in the case of SWNTs, due to their higher aspect ratio compared to PEDOT:PSS. (Li et al. 2007) The SWNTs have aspect ratio of around 1000 and so compared to spherical and larger PEDOT:PSS particles, (Leaf and Muthukumar 2016) the SWNTs adsorbed on the fiber will hence have a larger number of contacts and therefore a denser conductive network that can explain the

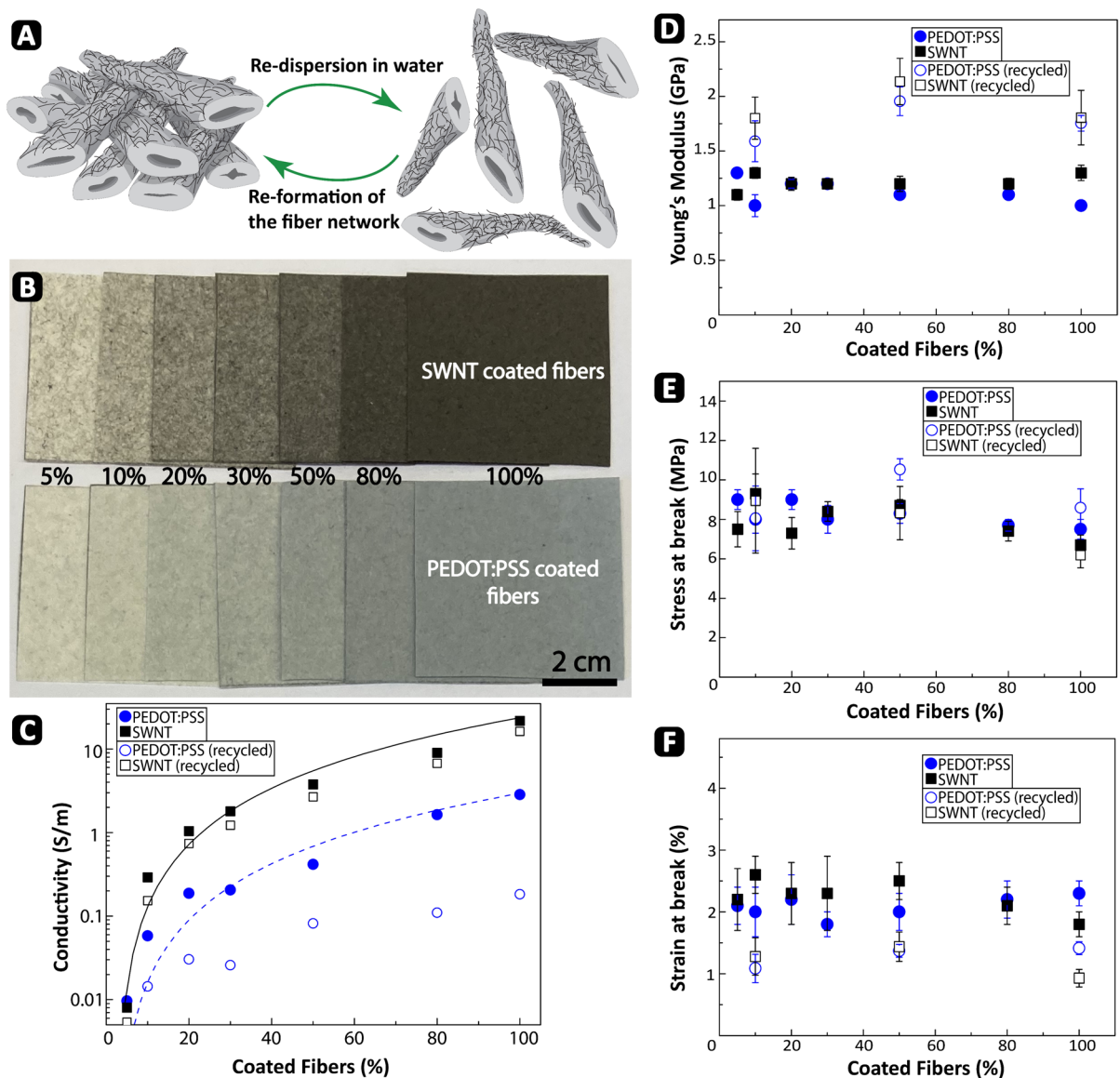


**Fig. 2** **A** A schematic showing the recycling process of the composite papers coated with SWNTs. **B** An optical image shows the composite papers; the fibers are either coated with SWNTs (top) or PEDOT:PSS (bottom). The composite papers made from 5 to 100% coated fibers. **C** Electrical conductivity of the composite papers before (filled symbols) and after recycling (hollow symbols). The experimental data were fitted

using the power law model (black curve for SWNTs and blue dashed curve for PEDOT:PSS papers before recycling). Tensile data showing: **D** Young's modulus, and **E** stress at break, **F** strain at break of the composite papers vs. coated fibers (%). The hollow symbols, also in this case, show the data for recycled papers

lower resistance of SWNT coated fibers, and consequently higher conductivity of the SWNT composite papers (see Table S1 and Fig. 2C). Since paper follows a random 2D network percolation, its conductivity should depend only on the conductivity of the individual fibers. To test this hypothesis, we measured the

conductivity of individually coated fibers to  $44 \pm 10$  kOhm/square for SWNT-coated fibers and  $361 \pm 31$  kOhm/square for PEDOT-coated fibers (see Table S1). These values indeed differ by around an order of magnitude indicating that the fiber–fiber contact resistance is negligible. Therefore, we considered an individually

coated fiber (with either SWNT or PEDOT:PSS) as the conductive unit and fitted the experimentally measured conductivity data with the power law model:

$$\sigma = \sigma_0(\phi - \phi_c)^t \quad \phi > \phi_c$$

Where  $\sigma$  is conductivity of the composite,  $\sigma_0$  is the conductivity of the paper with 100% coated fibers,  $\phi$  is the volume fraction of the conductive component (coated fibers),  $\phi_c$  is the percolation threshold (volume fraction) and  $t$  is the critical exponent (defined as 2 by Lyons et al. (Lyons et al. 2008) for similar fiber networks). By fitting this model to our experimental data (see Fig. 2C), the estimated percolation threshold was around 2% for the coated fibers which is relatively low for macroscopic fibers and comparable to that of nanocomposites (Li et al. 2007). Interestingly, the conductivity of the SWNTs composite papers did not change more than 8% after 10 folding cycles, upon complete folding to 180° and unfolding of the paper (see Figure S2). This is an indication for folding stability.

The tensile results in Fig. 2D–F show similar Young's modulus, stress at break and strain at break for different compositions. This suggests that the increased number of coated fibers in the compositions do not alter the ductility and mechanical performance of the paper. This advantage can be related to the low fraction (only 1 wt%) of the nanomaterials (PEDOT:PSS or SWNT) coated on the fiber and in the whole paper. Due to slightly shorter fibers (see Figures S3 and S4) of the starting material, however, the absolute mechanical properties of the papers are lower compared with traditional papers used for packaging and printing applications (Yoshihara and Yoshinobu 2014).

The advantage of this work is that recycling does not deteriorate or remove the adsorbed conductive materials on the fibers. To quantify this, we measured the conductivity of the composite papers before and after recycling (see Fig. 2C). The results showed similar conductivity values (particularly for SWNT coated fibers) after recycling, supporting the hypothesis that the nanomaterials strongly adhered to the fiber surface and were not washed away during the recycling process. We noticed a larger drop in conductivity for the recycled PEDOT:PSS papers which could be a result of the polymer aging in long contact with air (Shi et al. 2022). The conductivity of the

recycled paper is however still high enough for many applications and this process can be further optimized in future developments.

The composite papers can in summary be recycled without removing the electroactive materials from the recycled fibers. The tensile data of the recycled papers showed similar stress at break compared to the pristine composite papers, whereas there is 35–50% decrease in the strain at break while the Young's modulus even showed 40–70% increase. These changes in mechanical properties are known to occur for regular paper. This is, however, to our knowledge the first demonstration of a process which allows for industrial recycling of electrically interactive papers using conventional processing.

To further analyze not only the electronic but also the electrochemical properties of the SWNT-coated composite papers, we fabricated supercapacitors using the recycled papers as electrodes (see materials and methods, and Figure S5). Even after recycling, the supercapacitors showed good capacitance values reaching 40 F/g at lower scan rates, and around 5 F/g at higher scan rates (around 100 mV/s). These results are promising performance, considering that we have only 1 wt% SWNTs in the paper overall. These papers can then be used for recyclable batteries and supercapacitors. In the next step, we demonstrate Li and Na ion batteries.

To make the paper-based batteries, we first mixed 50% of the fibers (required to form the paper) with BP dispersion. Black phosphorus (BP) can be prepared as a negatively charged aqueous dispersion (see materials and methods) with atomically layered structure of phosphorus (P) atoms (Sun et al. 2014). P has the ability to react with both sodium and lithium ions making it a suitable component in batteries (Jin et al. 2020; Subramaniam et al. 2022). As shown in Fig. 1F and Fig. 3A, the BP network on the fiber does not appear to have many connection points, mainly due to the low aspect ratio of BP and its rather large particle diameter and the influence this has on the deposition process (Ondaral et al. 2010). Therefore, we exposed the BP coated fibers (after washing) to a SWNTs dispersion leading to an excess adsorption of SWNTs and hence an electrically conducting network among the BPs on the individual fibers. To further enhance the electrical conductivity of the paper formed from these treated fibers, they were mixed with another 50% of fibers

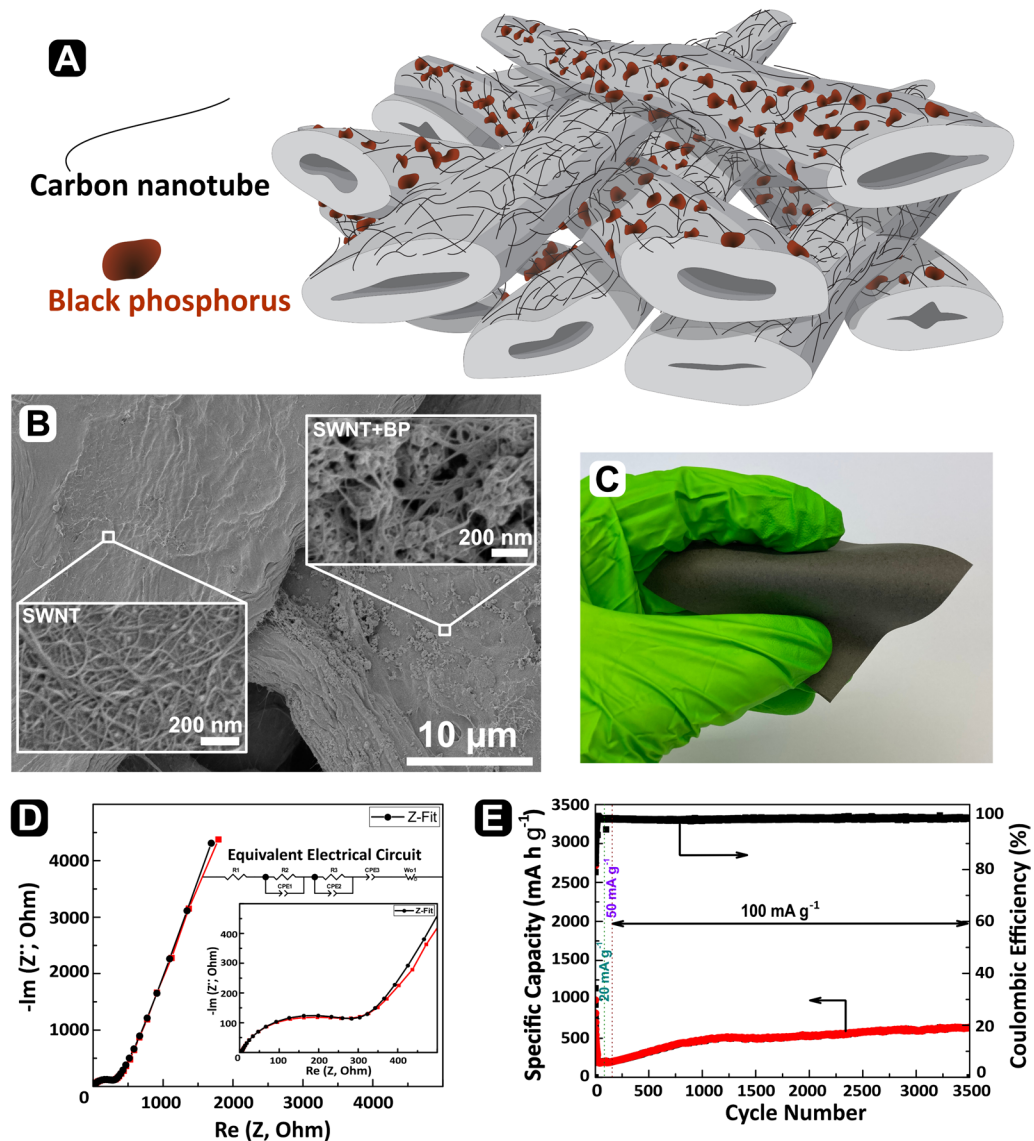


**Fig. 3** **A** Schematic showing a composite paper electrode where half of the fibers are coated with SWNTs and the other half coated with SWNT-BP. **B** SEM image showing a fiber contact between a BP-SWNT coated fiber acting as energy storage fiber and a pure SWNT coated fiber acting as a conductor. The higher magnification images from each fiber show the different surface morphologies. **C** Photo of an anode paper

coated with only the SWNT dispersion followed by washing and paper preparation. It should be remembered that in order to achieve a high cycling capacitance it is necessary to have a homogeneous, and electrochemically active structure, where the BP and the SWNTs form regular contacts in the

used for the batteries. **D** Nyquist plot showing impedance spectra of the composite paper at frequencies between 0.1 and 10 mHz. (The inset shows a zoomed-in section of the curve and equivalent electrical circuit), **E** 3500 cycles of charge/discharge for  $\text{Li}^+$ , in a half cell with the paper electrode at different rates

fiber–fiber joints. (Park and Sohn 2007) In these papers, the BPs are in contact through SWNTs on the nanoscale, and the BP+SWNT-coated fibers are in intimate contact with the electrical conductors, i.e. SWNT-coated fibers. The SEM image in Figs. 3B, S6 and S7 show an example of a randomly

distributed fiber contacts coated with different materials.

This approach is particularly interesting as the fibers should be coated and washed first, then mixed at a given composition to enable full control over the final composition of the functional materials in the composite paper. For instance, if we coat the cationic fibers with an aqueous dispersion containing 50/50 w/w BP and SWNT, we would end up with fibers of a different composition since the affinity of the separate nanomaterials to adsorb onto the fibers is different. This can be related to difference in diffusion and charge of the particles, which is apparent when comparing SWNTs and BPs (see Figure S8).

Another advantage of this method is that the BP and SWNT together constitute only 1 wt% of the entire paper. The high-performance at this low fraction can be related to the homogeneously coated individual fibers, as well as high number of fiber contacts in the paper. (Corte and Kallmes 1962; Yi et al. 2004).

The Nyquist plot shows the impedance behavior of the original composite paper as electrode against Li (see Fig. 3D) along with equivalent electrical circuit (Fig. 3D inset). The latter consisted of components: (i) at high frequency,  $R_1$  ( $=5.02$  Ohm) represent the resistance of Li migration in electrolyte and the separator; (ii) the damped semi-circle at the middle frequency represented with 2 similar groups in series to other with each containing resistances in parallel to constant-phase-elements, ( $R_2||CPE_1$ ,  $R_3||CPE_2$ , Fig. 3D inset). The latter group represents resistance-to-charge-transfer ( $R_{ct}=R_3=277.7$  Ohm) while former group accounts to resistance at the interfacial layer.; (iii) inclined line represents the Li mass diffusion at low frequency. Therefore, the electrically conductive paper exhibited low  $R_{ct}$  and hence, was tested as negative electrode for lithium-ion batteries between 0.002 and 3 V as shown in Fig. 3E. When tested for  $Li^+$  battery at  $20$  mA  $g^{-1}$ , the composite paper delivered a discharge capacity of  $2715.8$  mA h  $g^{-1}$  with an initial reversible 34.3% Coulombic efficiency (CE). This drastic irreversible first cycle loss could be due to formation of solid-electrolyte-interface layer at a lower voltage which entraps the lithium ions. (Zhang et al. 2006) The specific capacity, however, drops for a few initial cycles that is probably due to the slow diffusion of electrolyte into the interspaces of the rigid cellulose/SWNT networks which in turn

probably provided a high resistance-to-charge transfer (for more information see Figure S9). The results also show that the electrochemical performance slowly increases with cycle numbers at high current density of 50 and 100 mA  $g^{-1}$ . This increasing trend could be due to the enhanced electrolyte diffusion and an improved accessibility of active sites for ions and electronic transports within the cellulose fiber. (Dong et al. 2022) Overall, the composite paper batteries delivered a specific capacity of  $642$  mA h  $g^{-1}$  at 100 mA  $g^{-1}$  even after 3500 cycles with 99.5% CE which is a high performance for a no-additives free-standing electrode which could enable building an inexpensive and flexible battery for electronics. When tested as flexible anode for sodium ion battery (Figure S10), the electrochemical performance was par well in the initial cycle at  $20$  mA  $g^{-1}$  but deteriorates at 100 mA  $g^{-1}$  which might be due to the slow transport of  $Na^+$  owing to its large atomic radius and low electrochemical potential of sodium as compared to lithium.

These preliminary results can pave the way for using industrial paper making process for the fabrication of both  $Li^+$  as well as  $Na^+$  batteries. Even though the initial energy storage values are not in par with state-of-the-art batteries, we think these batteries can find application areas for example in printed electronics. (Cheng et al. 2013; Yao et al. 2017; Poulin et al. 2022).

## Conclusions

In summary, we were able to prepare conductive composite papers, using an industrially scalable chemical modification of the fibers, where cationic charges were covalently attached to the fibers in wet state. The charged fibers could subsequently adsorb negatively charged functional materials in water, ranging from conducting polymers, such as PEDOT:PSS, to nanomaterials such as CNTs, turning the wet fibers into electrically conductive paper. This process was fast and could easily be implemented as a part of paper making. The functionalized fibers could be used alone or in mixtures with other fibers in a conventional paper-making process to form a fundamentally new form of functional papers at scale. This is possible since the adsorbed components are not washed away from the fibers

during the paper dewatering process, and do not disrupt the formation of strong fiber–fiber joints that are necessary to form papers with acceptable mechanical properties. The joints can form a strong network and act as an efficient connection point for the electronic and ionic transport between the fibers. The conductive coated nanomaterials were strongly adsorbed onto the fibers and the paper could therefore be recycled without degrading the electrical function of the composite papers. This indicates that efficient fiber–fiber contacts are reformed after the recycling process. We also used these fibers to fabricate lithium and sodium ion paper batteries. In these paper batteries, half of the fibers were coated with black phosphorus (and carbon nanotubes) and the other half with only carbon nanotubes for increasing the conductivity of the formed paper. Future improvements should focus on increasing the strength of paper made from coated cationic fibers and to use other electroactive materials such as 2D materials, new generations of conducting polymers, or even active cellulose derivatives (Koga et al. 2022; Fukuhara et al. 2021).

The chemical modification of cationic fibers can also be done using industrial processes, such as kneading mixer machines (Willberg-Keyriläinen et al. 2019) and decreased water content to substantially increase the yield.

This work can open new possibilities for using industrial papermaking as a route towards future recyclable electroactive devices, such as capacitors, batteries, digital devices, and sensors. (Mirica et al. 2013; Lin et al. 2016; Hajian et al. 2019; Mogera et al. 2022; Yang et al. 2022).

**Acknowledgments** We would like to acknowledge Knut and Alice Wallenberg Foundation, and Vinnova through “Digital Cellulose Center” for funding. We thank Tobias Benselfelt for the graphics.

**Authors’ contribution** The manuscript was written through contributions by all authors. All authors reviewed the manuscript.

**Funding** Knut and Alice Wallenberg Foundation.

**Availability of data and materials** Not applicable

**Declarations**

**Conflict of interest** The authors have no competing interests

**Ethics approval and consent to participate** Not applicable.

**Consent for publication** Not applicable.

## References:

- Agarwal M, Xing Q, Shim BS, Kotov N, Varshneyan K, Lvov Y (2009) Conductive paper from lignocellulose wood microfibrils coated with a nanocomposite of carbon nanotubes and conductive polymers. *Nanotechnology* 20(21):215602. <https://doi.org/10.1088/0957-4484/20/21/215602>
- Berggren MD, Nilsson D, Robinson ND (2007) Organic materials for printed electronics. *Nat Mater* 6(1):3–5. <https://doi.org/10.1038/nmat1817>
- Brunetti F, Operamolla A, Castro-Hermosa S, Lucarelli G, Manca V, Farinola GM, Brown TM (2019) Printed solar cells and energy storage devices on paper substrates. *Adv Func Mater* 29(21):1806798. <https://doi.org/10.1002/adfm.201806798>
- Cheng Q, Song Z, Ma T, Smith BB, Tang R, Yu H, Jiang H, Chan CK (2013) Folding paper-based lithium-ion batteries for higher areal energy densities. *Nano Lett* 13(10):4969–4974. <https://doi.org/10.1021/nl4030374>
- Corte H, Kallmes O (1962) Statistical geometry of a fibrous network. The formation and structure of paper: 13–46 <https://doi.org/10.15376/frc.1961.1.351>
- Dong Q, Zhang X, Qian J, He S, Mao Y, Brozana AH, Zhang Y, Pollard TP, Borodin OA, Wang Y (2022) A cellulose-derived supramolecule for fast ion transport. *Sci Adv* 8(49):eadd2031. <https://doi.org/10.1126/sciadv.add2031>
- Fugetsu B, Sano E, Sunada M, Sambongi Y, Shibuya T, Wang X, Hiraki T (2008) Electrical conductivity and electromagnetic interference shielding efficiency of carbon nanotube/cellulose composite paper. *Carbon* 46(9):1256–1258. <https://doi.org/10.1016/j.carbon.2008.04.024>
- Fukuhara M, Kuroda T, Hasegawa F, Hashida T, Takeda M, Fujima N, Morita M, Nakatani T (2021) Amorphous cellulose nanofiber supercapacitors. *Sci Rep* 11(1):6436. <https://doi.org/10.1038/s41598-021-85901-3>
- Hajian A, Wang Z, Berglund LA, Hamed MM (2019) Cellulose nanopaper with monolithically integrated conductive micropatterns. *Adv Electron Mater* 5(3):1800924. <https://doi.org/10.1002/aelm.201800924>
- Hamed MM, Ainla A, Güder F, Christodouleas DC, Fernández-Abedul MT, Whitesides GM (2016) Integrating electronics and microfluidics on paper. *Adv Mater* 28(25):5054–5063. <https://doi.org/10.1002/adma.201505823>
- Ho TTT, Zimmermann T, Hauert R, Caseri W (2011) Preparation and characterization of cationic nanofibrillated cellulose from etherification and high-shear disintegration processes. *Cellulose* 18:1391–1406. <https://doi.org/10.1007/s10570-011-9591-2>
- Hu L, Cui Y (2012) Energy and environmental nanotechnology in conductive paper and textiles. *Energy Environ Sci* 5(4):6423–6435. <https://doi.org/10.1039/C2EE02414D>

- Hu L, Wu H, La Mantia F, Yang Y, Cui Y (2010) Thin, flexible secondary Li-ion paper batteries. *ACS Nano* 4(10):5843–5848. <https://doi.org/10.1021/nn1018158>
- Hu L, Choi JW, Yang Y, Jeong S, La Mantia F, Cui LF, Cui Y (2009) Highly conductive paper for energy-storage devices. *P Natl A Sci* 106(51):21490–21494. <https://doi.org/10.1073/pnas.0908858106>
- Hübler A, Trnovec B, Zillger T, Ali M, Wetzold N, Mingeback M, Wagenpahl A, Deibel C, Dyakonov V (2011) Printed paper photovoltaic cells. *Adv Energy Mater* 1(6):1018–1022. <https://doi.org/10.1002/aenm.201100394>
- Imai M, Akiyama K, Tanaka T, Sano E (2010) Highly strong and conductive carbon nanotube/cellulose composite paper. *Compos Sci Technol* 70(10):1564–1570. <https://doi.org/10.1016/j.compscitech.2010.05.023>
- Isacsson P, Wang X, Fall A, Mengistie D, Calvie E, Granberg H, Gustafsson GR, Berggren M, Engquist I (2020) highly conducting nanographite-filled paper fabricated via standard papermaking techniques. *ACS Appl Mater Inter* 12(43):48828–48835. <https://doi.org/10.1021/acsami.0c13086>
- Isacsson P, Jain K, Fall A, Chauve V, Hajian A, Granberg H, Boiron L, Berggren M, Håkansson K, Edberg J (2022) Production of energy-storage paper electrodes using a pilot-scale paper machine. *J Mater Chem A* 10(40):21579–21589. <https://doi.org/10.1039/D2TA04431E>
- Jin H, Xin S, Chuang C, Li W, Wang H, Zhu J, Xie H, Zhang T, Wan Y, Qi Z (2020) Black phosphorus composites with engineered interfaces for high-rate high-capacity lithium storage. *Science* 370(6513):192–197. <https://doi.org/10.1126/science.aav5842>
- Kaplan BY, Şanlı LI, Gürsel SA (2017) Flexible carbon–cellulose fiber-based composite gas diffusion layer for polymer electrolyte membrane fuel cells. *J Mater Sci* 52(9):4968–4976. <https://doi.org/10.1007/s10853-016-0734-6>
- Koga H, Nagashima K, Suematsu K, Takahashi T, Zhu L, Fukushima D, Huang Y, Nakagawa R, Liu J, Uetani K, Nogi M (2022) Nanocellulose paper semiconductor with a 3D network structure and its nano–micro–macro trans-scale design. *ACS Nano* 16(6):8630–8640. <https://doi.org/10.1021/acsnano.1c10728>
- Koklukaya O, Carosio F, Grunlan JC, Wagberg L (2015) Flame-retardant paper from wood fibers functionalized via layer-by-layer assembly. *ACS Appl Mater Inter* 7(42):23750–23759. <https://doi.org/10.1021/acsami.5b08105>
- Leaf MA, Muthukumar M (2016) Electrostatic effect on the solution structure and dynamics of PEDOT: PSS. *Macromolecules* 49(11):4286–4294. <https://doi.org/10.1021/acs.macromol.6b00740>
- Leijonmarck S, Cornell A, Lindbergh G, Wågberg L (2013) Single-paper flexible Li-ion battery cells through a paper-making process based on nano-fibrillated cellulose. *J Mater Chem A* 1(15):4671–4677. <https://doi.org/10.1039/C3TA01532G>
- Li J, Ma PC, Chow WS, To CK, TangKim BZJK (2007) Correlations between percolation threshold, dispersion state, and aspect ratio of carbon nanotubes. *Adv Funct Mater* 17(16):3207–3215. <https://doi.org/10.1002/adfm.200700065>
- Lin Y, Gritsenko D, Liu Q, Lu X, Xu J (2016) Recent advancements in functionalized paper-based electronics. *ACS Appl Mater Inter* 8(32):20501–20515. <https://doi.org/10.1021/acsami.6b04854>
- Lyons PE, De S, Blighe F, Nicolosi V, Pereira LFC, Ferreira MS, Coleman JN (2008) The relationship between network morphology and conductivity in nanotube films. *J Appl Phys* 104(4):044302. <https://doi.org/10.1063/1.2968437>
- Martinez AW, Phillips ST, Butte MJ, Whitesides GM (2007) Patterned paper as a platform for inexpensive, low-volume, portable bioassays. *Angew Chem Int Edit* 119(8):1340–1342. <https://doi.org/10.1002/anie.200603817>
- Mirica KA, Azzarelli JM, Weis JG, Schnorr JM, Swager TM (2013) Rapid prototyping of carbon-based chemiresistive gas sensors on paper. *P Natl A Sci* 110(35):E3265–E3270. <https://doi.org/10.1073/pnas.1307251110>
- Mogera U, Guo H, Namkoong M, Rahman MS, Nguyen T, Tian L (2022) Wearable plasmonic paper-based microfluidics for continuous sweat analysis. *Sci Adv* 8(12):eabn1736. <https://doi.org/10.1126/sciadv.abn1736>
- Nguyen TH, Fraiwan A, Choi S (2014) Paper-based batteries: a review. *Biosens Bioelectron* 54:640–649. <https://doi.org/10.1016/j.bios.2013.11.007>
- Ondaral S, Ankerfors C, Odberg L, Wagberg L (2010) Surface-induced rearrangement of polyelectrolyte complexes: influence of complex composition on adsorbed layer properties. *Langmuir* 26(18):14606–14614. <https://doi.org/10.1021/la1022054>
- Park CM, Sohn HJ (2007) Black phosphorus and its composite for lithium rechargeable batteries. *Adv Mater* 19(18):2465–2468. <https://doi.org/10.1002/adma.200602592>
- Pei A, Butchosa N, Berglund LA, Zhou Q (2013) Surface quaternized cellulose nanofibrils with high water absorbency and adsorption capacity for anionic dyes. *Soft Matter* 9(6):2047–2055. <https://doi.org/10.1039/C2SM27344F>
- Pettersson F, Keskinen J, Remonen T, von Hertzen L, Jansson E, Tappura K, Zhang Y, Wilén CE, Österbacka R (2014) Printed environmentally friendly supercapacitors with ionic liquid electrolytes on paper. *J Power Sources* 271:298–304. <https://doi.org/10.1016/j.jpowsour.2014.08.020>
- Picu RC (2011) Mechanics of random fiber networks—a review. *Soft Matter* 7(15):6768–6785. <https://doi.org/10.1039/C1SM05022B>
- Poulin A, Aeby X, Nyström G (2022) Water activated disposable paper battery. *Sci Rep* 12(1):11919. <https://doi.org/10.1038/s41598-022-15900-5>
- Przybysz K, Małachowska E, Martyniak D, Boruszewski P, Howska J, Kalinowska H, Przybysz P (2018) Yield of pulp, dimensional properties of fibers, and properties of paper produced from fast growing trees and grasses. *BioResour* 13(1):1372–1387. <https://doi.org/10.15376/biores.13.1.1372-1387>
- Shi Y, Zhou Y, Che Z, Shang J, Wang Q, Liu F, Zhou Y (2022) Degradation phenomena and degradation mechanisms for highly conductive PEDOT: PSS films. *Mater Lett* 308:131106. <https://doi.org/10.1016/j.matlet.2021.131106>

- Subramaniyam CM, Kang MA, Li J, VahidMohammadi A, Hamed MM (2022) Additive-free red phosphorus/Ti<sub>3</sub>C<sub>2</sub>T<sub>x</sub>MXene nanocomposite anodes for metal-ion batteries. *Energy Adv* 1(12):999–1008. <https://doi.org/10.1039/D2YA00168C>
- Sudheshwar A, Malinverno N, Hischer R, Nowack B, Som C (2023) The need for design-for-recycling of paper-based printed electronics—a prospective comparison with printed circuit boards. *Resour Conserv Recy* 189:106757. <https://doi.org/10.1016/j.resconrec.2022.106757>
- Sun J, Zheng G, Lee HW, Liu N, Wang H, Yao H, Yang W, Cui Y (2014) Formation of stable phosphorus–carbon bond for enhanced performance in black phosphorus nanoparticle–graphite composite battery anodes. *Nano Lett* 14(8):4573–4580. <https://doi.org/10.1021/nl501617j>
- Tobjörk D, Österbacka R (2011) Paper electronics. *Adv Mater* 23(17):1935–1961. <https://doi.org/10.1002/adma.201004692>
- Willberg-Keyriläinen P, Pitkänen P, Hulkko J, Asikainen M, Setälä H (2019) The effect of mixing and consistency on cellulose cationization. *Heliyon*. <https://doi.org/10.1016/j.heliyon.2019.e01349>
- Yamada K, Henares TG, Suzuki K, Citterio D (2015) Paper-based inkjet-printed microfluidic analytical devices. *Angew Chem Int Edit* 54(18):5294–5310. <https://doi.org/10.1002/anie.201411508>
- Yang P, Li J, Lee SW, Fan HJ (2022) Printed zinc paper batteries. *Adv Sci* 9(2):2103894. <https://doi.org/10.1002/advs.202103894>
- Yao B, Zhang J, Kou T, Song Y, Liu T, Li Y (2017) Paper-based electrodes for flexible energy storage devices. *Adv Sci* 4(7):1700107. <https://doi.org/10.1002/advs.20170107>
- Yi Y, Berhan L, Sastry A (2004) Statistical geometry of random fibrous networks, revisited: waviness, dimensionality, and percolation. *J Appl Phys* 96(3):1318–1327. <https://doi.org/10.1063/1.1763240>
- Yoshihara H, Yoshinobu M (2014) Effects of specimen configuration and measurement method of strain on the characterization of tensile properties of paper. *J Wood Sci* 60:287–293. <https://doi.org/10.1007/s10086-014-1398-y>
- Zhang SS, Xu K, Jow T (2006) EIS study on the formation of solid electrolyte interface in Li-ion battery. *Electrochim Acta* 51(8–9):1636–1640. <https://doi.org/10.1016/j.electacta.2005.02.137>

**Publisher's Note** Springer Nature remains neutral with regard to jurisdictional claims in published maps and institutional affiliations.

Springer Nature or its licensor (e.g. a society or other partner) holds exclusive rights to this article under a publishing agreement with the author(s) or other rightsholder(s); author self-archiving of the accepted manuscript version of this article is solely governed by the terms of such publishing agreement and applicable law.